 SDHM, vol.6, no.4, pp.289-303, 2010

# Closure Effect Evaluation of Surface Crack Growth under Cyclic Bending using S-FEM

**Masanori Kikuchi**[1] **and Kazuhiro Suga**[1]

**Abstract:** Crack closure effect on interaction of two surface crack growth processes by fatigue is studied. At first, change of C value in Paris' law along crack front of single surface crack is measured experimentally. It is shown that C value decreases near specimen surface. Crack closure effect is studied numerically for a surface crack by elastic-plastic cyclic analyses. It is found that closure effect appears more strongly near specimen surface than the maximum-depth point. By determining effective stress intensity factor including closure effect, it is shown that change of C value is equal to the change of closure effect along crack front. Using new C value considering closure effect, fatigue crack growth is predicted using S-FEM. It is shown that fatigue life and crack configuration agree well with experimental ones. Finally, interaction of two surface cracks is evaluated numerically, and it is shown that crack closure plays important role on the interaction of two cracks.

**Keywords:** Manuscript, preparation, typeset, format, SDHM.

## 1 Introduction

It is well know that final fracture of structure is mainly due to fatigue of materials by long-term cyclic loading. It is important to evaluate fatigue damage for the integrity of structures. For this purpose, estimation of residual fatigue life is a key technology after a small crack is detected. For the evaluation of residual fatigue life, FEM (Finite Element Method) plays an important role with some crack growth criteria. In the 2-dimensional field, comparisons of fatigue test results with those of numerical simulation have been done by many authors. The estimation of crack growth rate by fatigue is conducted using Paris' law(1), and crack growth direction is evaluated by MTS (Maximum Tangential Stress ) criterion(2). Availabilities of these criteria have been verified by many studies (3,4). In the 3-dimensional filed,

[1] Tokyo University of Science, Japan.

comparison of experiments with numerical simulation has been done in some literatures (5,6). But these comparisons have not been done well. It is because of problems on numerical simulation techniques. In 3-dimensional filed, modeling of 3-dimensional crack shape for FEM analysis is not easy when it changes it's shape continuously. Especially under mixed mode loading conditions, configuration of 3-d. fatigue crack becomes very complicated, and it is very time consuming work to model its' shape precisely. Recently, some new techniques solved this problem. For example, Portela et al.(7) simulated surface crack growth problem using Dual BEM. Kikuchi et al. simulated fatigue crack growth automatically using S-FEM(8,9) in 2- and 3-dimensional fields. Kikuchi et al. (10) also carried out fatigue test under mixed mode, Mode I+II+III, condition, and results are compared with numerical simulation. It is found that evaluation of crack closure effect during fatigue behavior is important to evaluate fatigue crack growth quantitatively.

In this study, fatigue test is conducted using surface crack specimen, and results are compared with those of numerical simulation. Crack closure effect is evaluated for surface crack problem, and crack aspect ratio is evaluated. Based on the comparison of experiment and numerical simulation, crack growth criterion in 3-d. filed is studied and it's availability is discussed. Finally, interaction of two surface cracks is evaluated numerically, and crack closure effect is discussed.

## 2 Coefficient C of Paris' Law

Crack growth rate by fatigue load is expressed by Paris' law(2) as follows.

$$\frac{da}{dN} = C\,(\Delta K)^n \tag{1}$$

where a is crack length, N is number of cyclic loadings and$\Delta K$ is stress intensity factor range in loading cycle. Coefficients C and n are material constants to determine fatigue crack growth rate. These values are determined by pure mode I fatigue test. Raju and Newman et al.(4) estimated the change of surface crack configuration assuming it changes as a semi-elliptical shape. Stress Intensity Factor is calculated by Newman-Raju equation (11) at the deepest point and surface point of a surface crack. They assumed coefficient C has different value at deepest point and surface of a surface crack, and crack growth rates are estimated at these 2 points, as follows.

$$\frac{da}{dN} = C_a\,(\Delta K_a)^n \tag{2}$$

$$\frac{dc}{dN} = C_c\,(\Delta K_c)^n \tag{3}$$

where $C_c$ and $C_a$ are coefficient C value in Paris' law at surface and deepest point of a surface crack, respectively. $\Delta K_c$ and $\Delta K_a$ are stress intensity factor ranges at surface and deepest point. In ref.(4), it is concluded that surface crack shape is well estimated numerically by assuming a relation between $C_c$ and $C_a$ by the next equation.

$$C_c = 0.9^n C_a \tag{4}$$

It means that coefficient C value of Paris' law changes along crack front of a surface crack. It is based on the assumption that surface crack may grow keeping its' shape as semi-elliptical one.

By S-version FEM, a fully automatic fatigue crack growth system was developed by one of authors (9), and it is shown that surface crack shape becomes different from semi-elliptical shape in some cases. By this method, stress intensity factor can be evaluated many points along crack surface, and crack growth rate should be determined at each point. It is necessary to know $C$ value along surface crack front. If it changes along the crack front, it is necessary to know how it changes along the crack front.

In the following, pure mode I fatigue test is conducted using surface cracked specimen, and crack growth rate and change of surface crack shape are obtained. Same problem is simulated using S-version FEM, and stress intensity factor, KI, along crack front is calculated. Change of C value along crack front is studied and discussed.

## 3 Fatigeu Test of Surface Cracked Specimen

Aluminum alloy A2017-T3 is used as test specimen. Material constants of this material are shown in Table 1. Shape of specimen is shown in Fig.1, where S=140mm, B=50mm and t=15mm. At the center of the specimen, single surface crack is introduced by fatigue. Initial aspect ratio of this surface crack is 0.9. Cyclic load is subjected by three-point bending. Stress ratio R=0.1, and R is changed to 0.8 for the marking of crack shape by introducing beach marks.

Figure 2 shows crack surface after fatigue test. Beach marks are clearly observed and crack growth rate is obtained by measuring these beach mark spacing by referring number of cyclic loadings in each beach mark. Figure 3 shows the definition of eccentric angle which is used to show the position along the crack front. Eccentric angle $\theta = 0^\circ$ and $\theta = 180^\circ$ show surface of specimen, and $\theta = 90^\circ$ means the deepest point of surface crack.

By measuring each beach mark configuration, FEM model is made for each crack shape, and stress intensity factor, $K_I$, is calculated along crack front. Figure 4 shows

Table 1: Material properties of A2017-T3

| Young's modulus | Yield stress | Tensile strength |
|---|---|---|
| 70.2[GPa] | 333[MPa] | 418[MPa] |

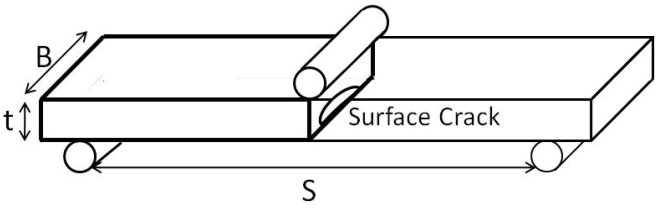


Figure 1: Three point bending specimen

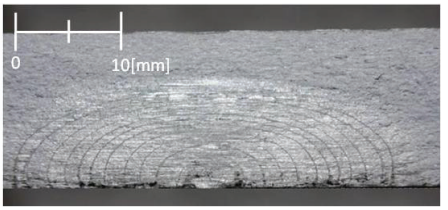


Figure 2: Beach mark

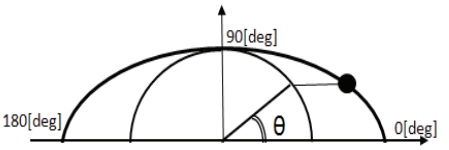


Figure 3: Definition of eccentric angle

relation between $\Delta K$ and crack growth rate per each cycle, da/dN. By referring Fig.3, it is noticed that location on the crack front for $\theta = 60^\circ$ and $\theta = 120^\circ$ are symmetric with respect to center line. Data of these two locations are plotted by using same marks. Data are obtained for each $10^\circ$ from $\theta = 0^\circ$ to $\theta = 180^\circ$. Results from 4 locations along crack front are shown in Fig.4. Three specimens are tested by the same way, and averaged data of these three specimens are shown in Fig.4. It is noticed that data of $\theta = 0^\circ$ and $\theta = 180^\circ$ are different from other data. Except these data, whole data show similar results. C and n values are measured from these data and results are shown in Table 2. n value scatters a little, about $\pm 10\%$. The average value of it is n=2.93. Using this average n value, C value is evaluated again.

Figure 5 shows results. The abscissa of Fig.5 is eccentric angle, and ordinate is C value. C value changes largely from $\theta = 0^\circ$ to $\theta = 40^\circ$, and decreases gradually to the deepest point of surface crack. By this result, C value at the deepest point is assumed to be $C_c$ value in equation (4), and $C_a$ value is calculated. They are also

plotted in Fig.5. $C_a$ value is very similar to C value at the surface. It means that the change of C value at the deepest point and surface by this experiment qualitatively agrees with results of Newman et al.

Table 2: C and n values by experiments

| $\theta$[deg] | $C[10^{-10}]$ | $n$ |
|---|---|---|
| 0 | 0.28 | 3.12 |
| 10 | 1.68 | 2.67 |
| 20 | 1.92 | 2.89 |
| 30 | 2.74 | 2.72 |
| 40 | 2.84 | 2.69 |
| 50 | 1.69 | 2.85 |
| 60 | 1.23 | 2.99 |
| 70 | 1.27 | 3.02 |
| 80 | 0.82 | 3.15 |
| 90 | 0.55 | 3.20 |

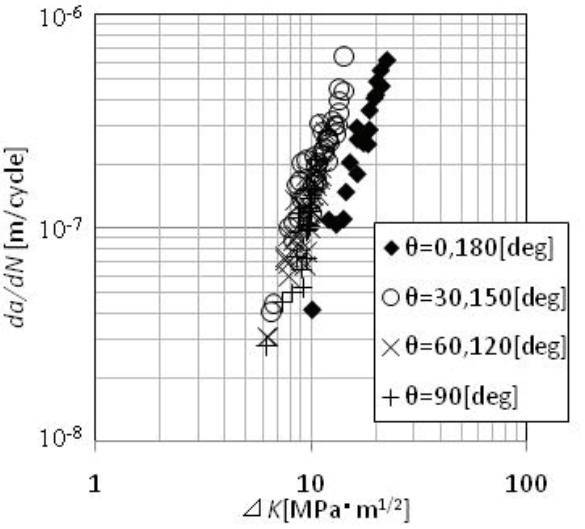


Figure 4: *da/dN*-Δ*K* curve

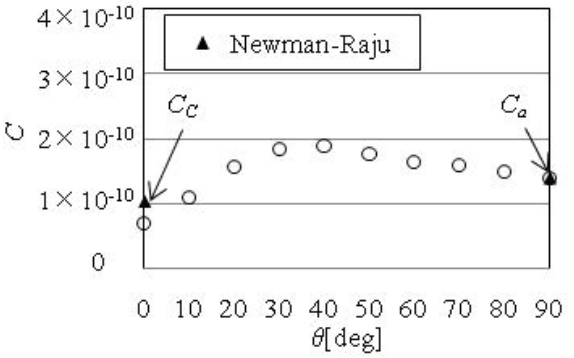


Figure 5: C values in each eccentric angles

## 4 Evaluation of Closure Effect at Crack Tip

In one of authors' previous paper(10), it is shown that crack shape is well estimated by considering crack closure effect for through crack problem. Effective stress intensity factor range, $\Delta K_{eff}$, is used instead of $\Delta K$ in Paris' law.

For surface crack problem, crack closure effect is evaluated in the following. Crack closure effect appears by elastic-plastic deformation at the crack tip. For elastic-plastic analysis, FEM model is made. Two beach marks in Fig.3 are chosen, and they are called beach mark A and B, as shown in Fig.6. Using their shapes, FEM model is made as shown in Fig.7. Very fine meshes are used between beach mark A and B, and there are 50 small meshes between them. Initial crack front shape is as same as that of beach mark A. Cyclic load is given which is same as stress intensity factor range, $\Delta K$, is equal to 10MPam$^{1/2}$, which is same with experiment. In each cyclic loading, elastic-plastic analysis and crack growth simulation are conducted using ANSIS. Stress-strain relation in plastic region is modeled by bi-linear relation, where hardening ratio H is assumed to be E/10. Figure 8 shows stress-strain relation of the material and bi-linear model.

Crack grows one mesh length, about 9.0-12.0$\mu$m, in each loading-unloading cycle. Crack growth is simulated by releasing constraints at the crack tip node, and closure is evaluated by the displacement at crack tip node. After closure at crack tip node, displacement of this node is constrained for further simulation. Crack growth rate depends on mesh size at the crack tip. But it is not a serious problem because Jiang et al.(12) found that crack closure behavior does not depend on crack tip mesh size largely. After 15 cyclic simulations, crack closure behavior saturates. In this study, crack closure is evaluated after 20 cyclic simulations.

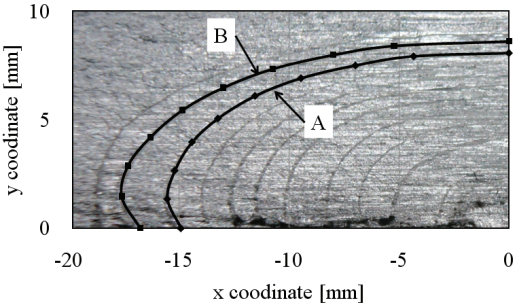


Figure 6: Crack shape

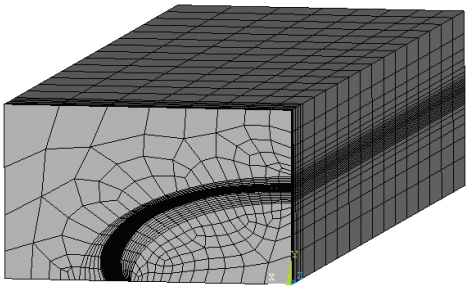

Figure 7: Mesh pattern for FEM analysis Fig.8 Stress-strain curve

Changes of crack opening-closure behaviors after 20 cycles are shown in Fig.9(a). The abscissa of this figure is eccentric angle of surface crack, and ordinate is COD (Crack Opening Displacement) for 3 load levels shown in Fig.9(b). COD is measured at crack tip node which is the nearest to the crack tip. At the maximum loading point, (P1 in Fig.9(b)), crack opens along whole crack front. COD is the maximum at surface of the specimen. After some amount of unloading (P2), crack closure occurs at first at specimen surface. After then, crack closure occurs gradually from specimen surface to deeper point along crack front. At each point, load at closure is called $P_{close}$, and closure rate U is defined by next equation.

$$U = \frac{P_{\max} - P_{close}}{\Delta P} \tag{5}$$

where $\Delta P$ is $0.9P_{max}$ because stress ratio is 0.1.

Figure 10 shows changes of U along crack front. U becomes the minimum value at

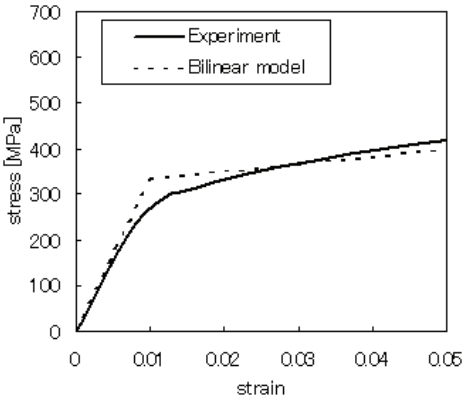


Figure 8: Stress-strain curve

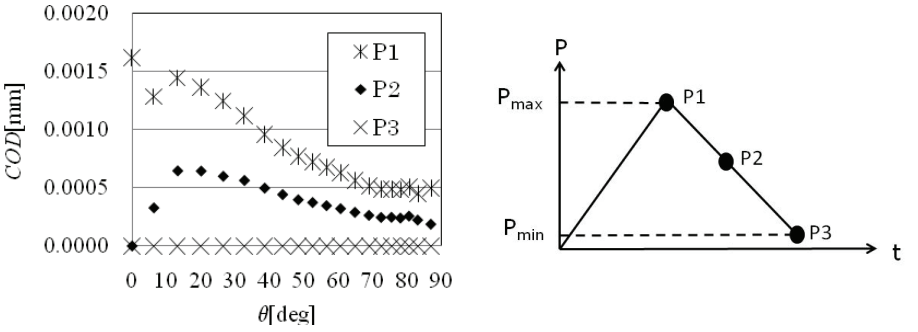


(a) Crack opening displacements (b) Corresponding loads

Figure 9: Changes of crack opening displacements

specimen surface, and increases rapidly to $\theta = 40^{\circ}$, and gradually decreases to the deepest point of surface crack. This is similar to the change of C value, shown in Fig.5.

Effective stress intensity factor range, $\Delta K_{eff}$, is defined by Eq.(6), and Paris' law is expressed by Eq.(7).

$$\Delta K_{eff} = \Delta K_{\times} U \tag{6}$$

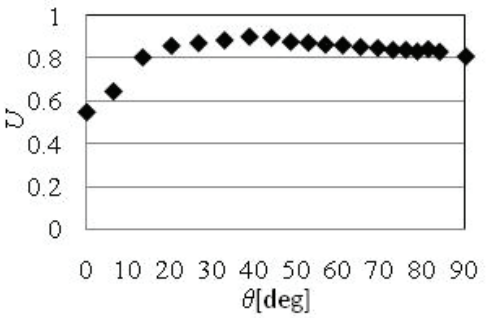


Figure 10: Changes of $U$ value

$$\frac{da}{dN} = C'(\Delta K_{eff})^n = C'(U\Delta K)^n \tag{7}$$

where coefficient C is expressed by $C'$ to distinguish from C value in Eq.(1). Comparing Eq.(7) with Eq.(1), relation between C and C' is obtained as follows.

$$C = C' \times U^n \tag{8}$$

Eq.(8) means that an apparent change of C value observed in experiment is due to the difference of crack closure effect along crack front.

Figure 11 shows relation between *da/dN* and $\Delta K_{eff}$, which is defined by Eq.(8). Strictly speaking, U value may change by the change of crack shape. But it is not practical to repeat elastic-plastic and crack growth simulation for new crack shapes. In this study, same U value is used for whole crack growth processes. From this figure, coefficient C' value is evaluated again by assuming that n value is same as 2.93. Results are shown in Fig. 12. Comparing with Fig.5, it is noticed that C' doesn't change largely along the crack front, and keeps nearly constant value. The average value of C' along crack front is C'=$2.65\times10^{-10}$.

Equation (8) means that apparent change of C value, shown in Eq.(4), is due to the effect of crack closure behavior.

The first section should be labeled Abstract; and should contain a brief description of the contents of the paper. The section of abstract should not be numbered. Subsequent sections should be numbered consecutively in arabic numbers, starting from 1.

Level one headings for sections should be in bold; and be flushed to the left. Level one heading should be numbered using arabic numbers, such as 1, 2, ....

Level two headings for subsections should be in bold-italic; and be flushed to the

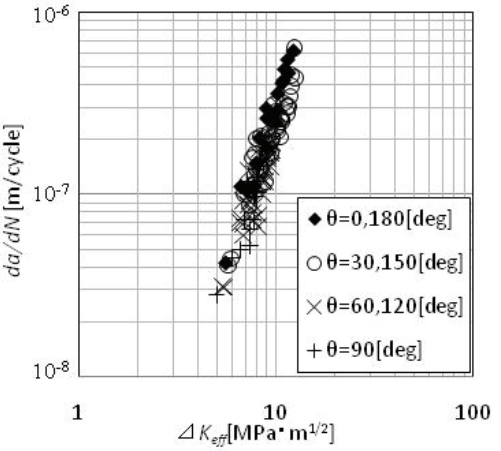


Figure 11: $da/dN - \Delta K_{eff}$ curve

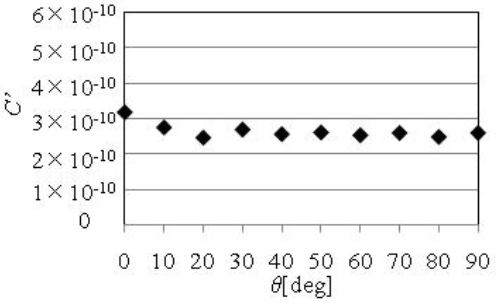


Figure 12: C' value in each eccentric angle

left. Level two headings should be numbered after the level one heading. For example, the second level two heading under the third level one heading should be numbered as 3.2.

Level three headings should be in italic; and be flushed to the left. Similarly, the level three headings should be numbered after the level two headings, such as 3.2.1, 3.2.2, etc.

## 5 Crack Growth Simulation and Experiment

Using n and average C' values, fatigue crack growth simulation is carried out using S-version FEM. Surface crack configurations are shown in Fig.13, where experi-

mental data are shown by solid line. Numerical results considering U effect are shown in the figure with results without considering U effect. By considering U effect, crack shape becomes near to experimental one especially at near specimen surface. It is concluded that crack shape is well estimated by considering crack closure effect.

Figure 14 shows relation between fatigue cycles and crack length at surface. The abscissa is increment of crack length at surface, and ordinate is number of cycles. Estimated results with and without considering U effects are compared with experimental ones. It is obvious that estimation without considering U effect evaluates crack growth rate much faster than experiment. It is conservative evaluation. But it seems too conservative. Results with U effect are also safe estimation. They are near to experiments and about 8% underestimate number of cycles. It is shown that fatigue life is accurately estimated by considering crack closure effect.

Two different types of styles can be used for equations and mathematical expres-

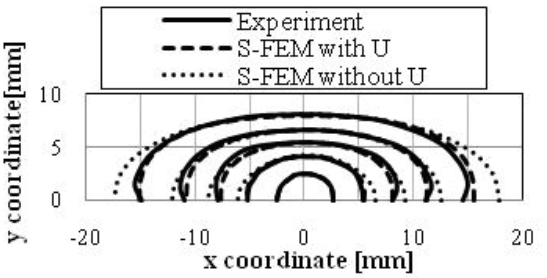


Figure 13: Changes of surface crack configurations

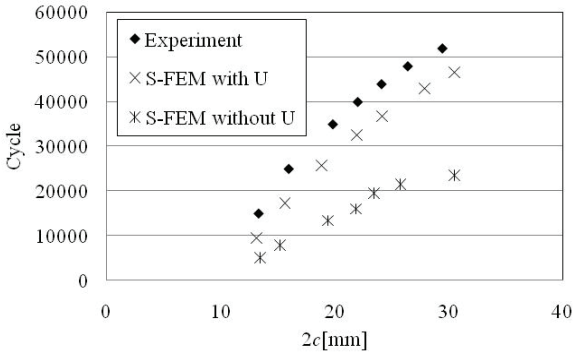


Figure 14: Fatigue cycles vs crack length at surface

sions. They are: in-line style, and display style.

## 6 Interaction of two surface cracks

Figure 15 shows two surface cracks in a plate. Distances between two crack tips are expressed by S and H, where S is a distance on horizontal line, and H is along vertical line. In such case, interaction effect of two cracks should be evaluated. By JSME code (13), two cracks are assumed to be a virtual single crack when both cracks grow and S value becomes zero or minus value.

In the following, these two cracks are evaluated using the same method shown before. The initial cracks are assumed to be the same sizes, $2c_1=2c_2=5$mm and $a_1=a_2=2$mm. Initial aspect ratio is 0.8. S and H are assumed to be 3mm.

Figure 16 show changes of crack shapes of two cracks for three N values. Similar to one of authors' previous paper (9), two cracks grow at first on its' plane, and change growth direction after inner crack tips overlapping. In these simulations, crack closure effect is considered. Distribution of U, shown in Fig.10, is used for theses cracks. Interaction effect on U distribution is not considered.

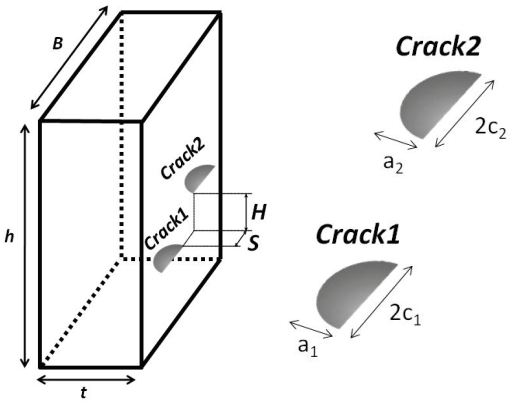


Figure 15: Model of two parallel cracks with different level.

Relations between crack length at surface, 2c, and number of cycles are shown in Fig.17. The abscissa of this figure is summation of increments of two crack lengths along horizontal line, and ordinate is number of cycles. In this figure, results of 2 cracks simulations and virtual single cracks after overlapping are shown for 2 cases, with and without considering U effect. Estimation of crack growth without

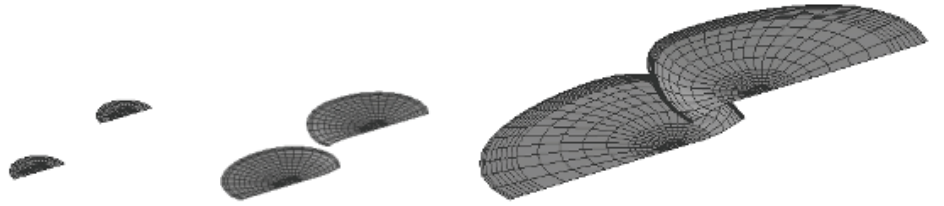

(a)N=0. (b) N=150000 (c)N=300000

Figure 16: Crack growth processes.

U effect underestimates number of cycles largely. Though it is conservative evaluation, it is too conservative. For example, cracks for N=150000 cycles are shown in Fig.18. Figure 18 (a) shows two cracks by considering U effect. Inner cracks overlap a little. But for the same cycles, two cracks are estimated largely if U effect is neglected, as shown in Fig.18(b), where crack overlapping occurs largely, and crack size is much larger than that of Fig 18(a). It is important to evaluate U effect properly to avoid too much conservative evaluation of fatigue crack growth.

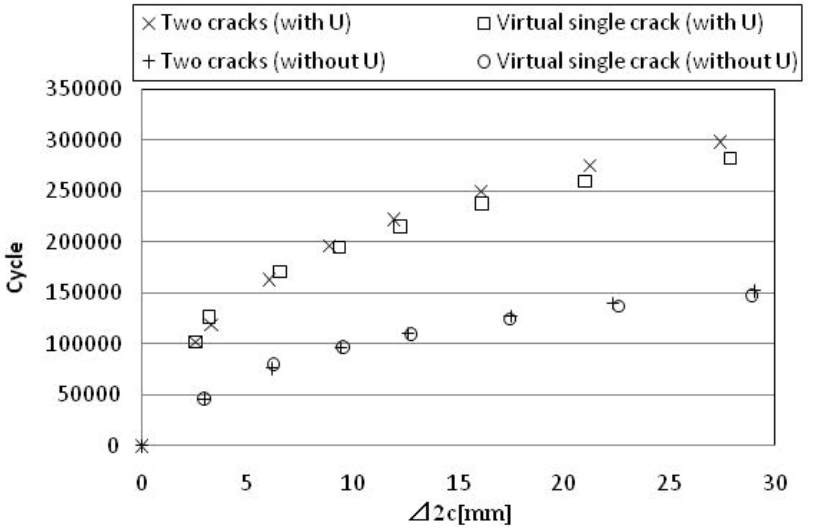


Figure 17: Crack length increment and number of cycles.

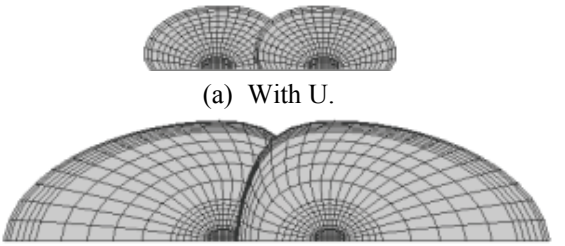

(a) With U.

(b) Without U.

Figure 18: Crack shapes for N=1500000 cycles.

## 7 Summary

It is pointed out that apparent change of the coefficient C value in Paris' law is due to the change of closure effect along surface crack. To estimate crack shape and crack growth process, it is important to consider closure effect not only for single crack but also for evaluation of interaction between two cracks.

## References

**Buchholz. F.-G.** (1994): Analysis of a 3D Mixed-Mode Fracture Problem by Virtual Crack Closure Integral Methods, Fracture Mechanics (Eds. A.V. Krishna Murthy, F.-G. Buchhloz), Proc. of the Indo-German Workshop on Advances in Fracture Mechanics, Indian Institute of Science, Bangalore, India, pp.7-12.

**Buchholz, F.-G., Richard, H.A.** (2004): Comparison of Computational Crack Path Predictioins with Experimental Findings for SEN-Specimens under Different Loadings, CD-ROM, Proc. of WCCM VI.

**Citarella, R., Buchholz, F.-G.** (2008): Comparison of crack growth simulation by DBEM and FEM for SEN-specimens undergoing torsion or bending loading, *Engineering Fracture Mechanics*, vol. 75, pp.489-509.

**dell'Erba D. N., Aliabadi M. H.** (2000): On the solution of three-dimensional thermo-elastic mixed-mode edge crack problems by the dual boundary element method, *Engineering Fracture Mechanics*, vol. 66, pp. 269-285.

**Erdogan, F., Sih, G.C.** (1963): On the Crack Extension in Plates Under Plane Loading and Transverse Shear, *Journal of Basic Engineering Transactions ASME*, Vol.85, pp.519-527.

**Jiang, Y. , Feng, M., Ding F.** (2005): A re-examination of plasticity-induced crack closure in fatigue crack propagation, *International Journal of Plasticity*, vol.21, pp.

1720-1740.

**JSME S Nal-2004** (2004): Codes for Nuclear Power Generation Facilities (in Japanese) pp.E-2-5.

**Kikuchi, M., Wada, Y., Takahashi, M., Li Y.** (2008): Fatigue crack growth simulation using S-FEM, *ASME PVP2008-61900*, Proc. ASME PVP2008.

**Kikuchi, M., Wada, Suyama, H., Li Y.** (2009): Interaction Effect Analysis of Two Surface Cracks Using S-Version FEM, *ASME PVP2009-77103,* Proc. ASME PVP2009.

**Maitiretimu, M., Kikuchi, M., Geni M.** (2009): Comparison of Experimental and Numerically Simulated Fatigue Crack Propagation, *Transactions of the Japan Society of Mechanical Engineers, Series A*, Vol.3, No.7, pp.952-967.

**Newman, J.C., Raju, I.S.** (1981): An Empirical Stress-Intensity Factor Equation for the Surface Crack, *Engineering Fracture Mechanics* Vol.15,No.1-2, pp.185-192.

**Newman J. C. Jr., Raju I. S.** (1979): Analyses of surface cracks in finite plates under tension or bending loads, *NASA*, TP-1578.

**Paris P, Erdogan F** (1963): A critical analysis of crack propagation laws, *Journal of Basic Engineering Transactions ASME*, pp.528-534.

**Portela A. et al.** (1992): The Dual Boundary Element Method : Effective Implementation for Crack Problems, *International Journal* for *Numerical Methods in Engineering*, vol.33, pp.1269-1287.

**Qing-fen, L., Gui-ying, Q., Sheng-yuan, Y., Buchholz, F.-G.** (2008): Computationla Fracture Analyses of a Compact Tension Shear Specimen with an Inclined Crack Plane, *Key Engineering Materials*, Vols. 385-387, pp.741-744.

**Raju I. S., Newman J. C. Jr.** (1979): Stress-Intensity Factors for a wide range of Semi-Elliptical Surface Cracks in Finite Thickness Plates, *Engineering Fracture Mechanics*, Vol.11, pp.817-829.